The Astrophysical Journal Letters, 767:L7 (5pp), 2013 April 10 doi:10.1088/2041-8205/767/1/L7

ON THE SIZE, SHAPE, AND DENSITY OF DWARF PLANET MAKEMAKE

M. E. Brown
Division of Geological and Planetary Sciences, California Institute of Technology, Pasadena, CA 91125, USA; mbrown@caltech.edu
Received 2013 January 24; accepted 2013 March 6; published 2013 March 25

ABSTRACT

A recent stellar occultation by the dwarf planet Makemake provided an excellent opportunity to measure the size and shape of one of the largest objects in the Kuiper belt. The analysis of these results provided what were reported to be precise measurements of the lengths of the projected axes, the albedo, and even the density of Makemake, but these results were, in part, derived from qualitative arguments. We reanalyzed the occultation timing data using a quantitative statistical description, and, in general, found the previously reported results on the shape of Makemake to be unjustified. In our solution, in which we use our inference from photometric data that Makemake is being viewed nearly pole-on, we find a 1σ upper limit to the projected elongation of Makemake of 1.02, with measured equatorial diameter of 1434 $\pm$ 14 km and a projected polar diameter of 1422 $\pm$ 14 km, yielding an albedo of $0.81^{+0.01}_{-0.02}$. If we remove the external constraint on the pole position of Makemake, we find instead a 1σ upper limit to the elongation of 1.06, with a measured equatorial diameter of 1434^{+48}_{-18} km and a projected polar diameter of 1420^{+18}_{-24} km, yielding an albedo of $0.81^{+0.03}_{-0.05}$. Critically, we find that the reported measurement of the density of Makemake was based on the misapplication of the volatile retention models. A corrected analysis shows that the occultation measurements provide no meaningful constraint on the density of Makemake.

Key words: Kuiper belt objects: individual (Makemake) – planets and satellites: atmospheres – planets and satellites: formation – methods: statistical

Online-only material: color figures

1. INTRODUCTION

The density of a solar system body is one of the most important parameters for understanding the composition, evolution, and formation history of the object. In the Kuiper belt, the wide range of densities, from below that of water ice to that of nearly pure rock, is one of the mysteries that continues to have no satisfactory explanation. Brown (2012) proposed several classes of general solutions to explain, in particular, the wide range of densities of objects in the dwarf planet size range. In one limiting scenario, densities gradual increase with size as small amounts of ice are removed with each accretional impact. In the other limit, the densities of the largest objects are stochastically set by single giant impacts which can remove significant quantities of ice and lead to one or more satellites with a small fraction of the mass of the primary. The density of Makemake could be a key discriminator between these types of models. Makemake is the largest known Kuiper belt object for which no satellite has been detected (Brown et al. 2006; Brown 2008). In that case, Makemake might never have suffered a density-increasing giant impact, and thus could have a density lower than the typical values of $\sim$2.1 g cm^{-3} and higher that appear typical for dwarf planets with small satellites. In contrast, a density $\gtrsim$2.1 g cm^{-3} for Makemake would indicate the correlation between high densities and the presence of collisional satellites is a mere coincidence unrelated to formation.

Ortiz et al. (2012, hereafter O12) measured a stellar occultation of Makemake and, from these data, infer a density of 1.7 ± 0.3 g cm^{-3} for the object. Such a density would strongly support the classes of models in which the high densities of objects such as Haumea and Eris are due to single giant impacts which left small moons in orbit. Because of the importance of this density for constraining the formation pathways of these icy dwarf planets, we investigate this density measurement to determine its robustness. To do so we reanalyze the occultation data of O12 using a quantitative, rather than qualitative, statistical framework. In addition to examining the density, this new analysis allows us to obtain statistically justifiable constraints on the size, shape, and albedo of Makemake for the first time.

2. OBSERVATIONS AND SPHERICAL FITTING

Makemake occulted the star NOMAD 1181-0235723 on 2011 April 23. O12 report eight detections of the occultation from stations in Chile and Brazil, and they fit square-well occultation models to determine the time of stellar disappearance and reappearance for each station, as well as uncertainties. The data quality are exquisite, with event uncertainties as small as 0.04 s in the best case, corresponding to chord lengths with uncertainties of only a few kilometers. As seen in Figure 1, however, one difficulty with the data is that five of the eight chords sample nearly the same region on Makemake and the three remaining stations sample identical chords 300 km south (Figure 1). The lack of strong constraint on the north–south dimension dominates the shape results of O12.

To determine the shape and density of Makemake, O12 first fit the data using simple χ^2 minimization and then present a series of qualitative arguments based on additional consideration to modify the results given by the data. Such an approach need not remain qualitative but can be given statistical meaning by adopting a Bayesian approach. We develop such an approach here.

To check for consistency with O12, we first attempt to reproduce their basic results and determine the best-fit model to describe the data assuming that Makemake is perfectly spherical. In this case we fit three parameters: the sphere diameter, d, and the x and y offset of the shadow of Makemake from the center of the predicted path. In our analysis we calculate

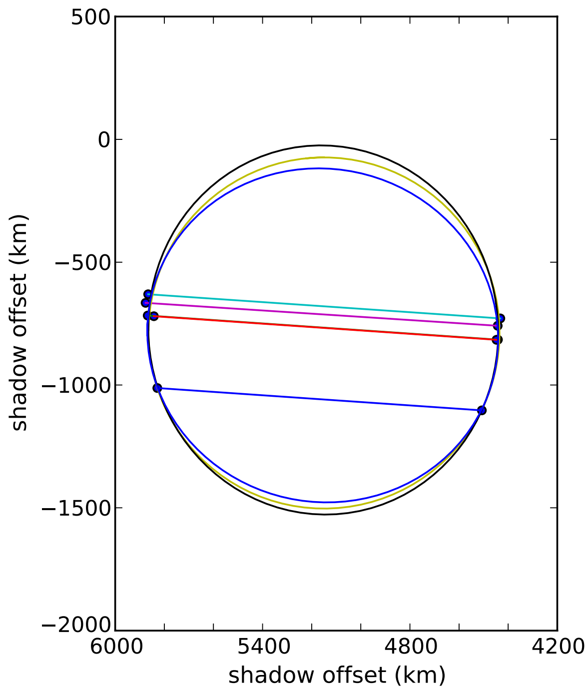

Figure 1. Projected locations of the stellar disappearance and reappearance at each of the observing stations. The lack of stations farther north and south leads to weak constraints on the elongation in that direction. We show the best-fit circular shadow, with a diameter of 1430 ± 7 km, as well as shadows with the 1σ maximum elongations allowed when using the density prior.

(A color version of this figure is available in the online journal.)

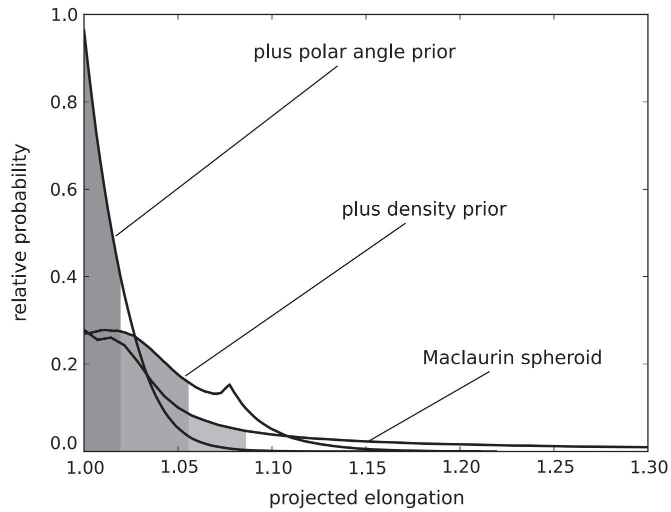

Figure 2. PDF of the projected elongation. The gray shaded regions show the 1σ regions containing 68.2% of the probability density. While the Maclaurin spheroid constraint yields a long tail to large projected elongations, adding the density prior with a lower limit of 1.3 g cm^{-3} limits the maximum true elongation and thus the projected elongation. A prior on the polar angle assuming a nearly pole-on view of Makemake yields even smaller projected elongations.

predicted disappearance and appearance times at each station given values of d, x, and y, and we compute the likelihood, which is identical to the value of χ^2 as described in O12, for those parameters. To compute the Bayesian probability function, we multiply the likelihood by the priors on all of the parameters. To begin, we assume simple uniform priors in x, y, and d for best comparison to O12.

To determine the probability distribution function (PDF) for each of the parameters, we integrate through phase space using a Markhov Chain Monte Carlo (MCMC) scheme. We use the Python package *emcee* (Foreman-Mackey et al. 2012) which implements the Goodman & Weare (2010) affine invariant ensemble sampler for MCMC. For our simple spherical fit, we found good convergence using an ensemble of 100 chains running 10^4 steps with an initialization ("burn-in") period, which is discarded, of 10% of the total length of each chain. The x and y offsets of the star are of no interest, so we treat them as nuisance parameters and marginalize over their distributions. The distribution of d—that is, the PDF marginalized over the other two parameters—is nearly Gaussian, and we find that the spherical diameter is 1430 ± 7 km. Throughout this Letter we define the best fit as the peak of the PDF and the 1σ range as the smallest region about the best fit containing 68.2% of the probability. If the peak of the PDF is at or near one of the extrema we report an upper or lower limit with the same method. The modest improvement in the uncertainty from the O12 result of 1430 ± 9 km is the result of the marginalization and is a small demonstration of the usefulness of this technique.

3. ELLIPSOID FIT

As correctly pointed out by O12, given plausible densities and the measured 7.77 hr spin period of Makemake (Heinze & de Lahunta 2009), the true shape of Makemake will not be a sphere, but rather a Maclaurin spheroid with an elongation dependent on the density and spin rate (Chandrasekhar 1969). Such a spheroid, viewed in projection, will appear as an ellipse. O12 fit directly to an elliptical shape and find, not surprisingly, that their best-fit ellipse is elongated in the north–south direction, with an axial ratio of 1.15 ± 0.17. They then argue that a true elongation in the north–south direction would be coincidental and that the real elongation is probably smaller. Qualitative arguments are given to suggest a "preferred" elongation of 1.05 ± 0.03, though the reasons for these precise values are unclear.

These arguments can be approached statistically rather than qualitatively. Rather than fitting an ellipse to the projected shape of the body, we fit to the full Maclaurin spheroid shape. We parameterize this shape with four parameters, E, the ratio of the equatorial diameter to the polar diameter, d, the polar diameter, ϕ, the angle of the pole with respect to the line of sight (which we call the "polar axis angle"), and, θ, the position angle of the largest dimension of the projected ellipse (the "azimuthal angle"). Such a fit has many degeneracies; these degeneracies, rather than being a problem, correctly account for the volume of phase space in the multi-dimensional fit and give a correct accounting of the probabilities of each of these parameters.

In our ellipsoid fit, we constrain the ratio of the polar to equatorial diameters to be between 1 and 1.716, the minimum and maximum values obtainable by a Maclaurin spheroid (Chandrasekhar 1969; we add additional constraints on the shape below). We add no constraints on the azimuth angle, and we choose ϕ such that the polar axis is oriented arbitrarily in space (we also modify this constraint below). Because of the much larger phase space to be explored, we run our MCMC sampler with an ensemble of 100 chains sampled through 10^5 iterations.

We find that the PDF of the elongation, E, is not highly constrained. The PDF for E peaks at $E = 1.03$ and decreases to 20% of the peak value by 1.716. The 1σ upper limit on the true elongation is 1.37. The projected elongation, is, however, more tightly constrained. The PDF peaks at 1.0 and has a 1σ upper limit of only 1.09 (Figure 2). Simply by correctly

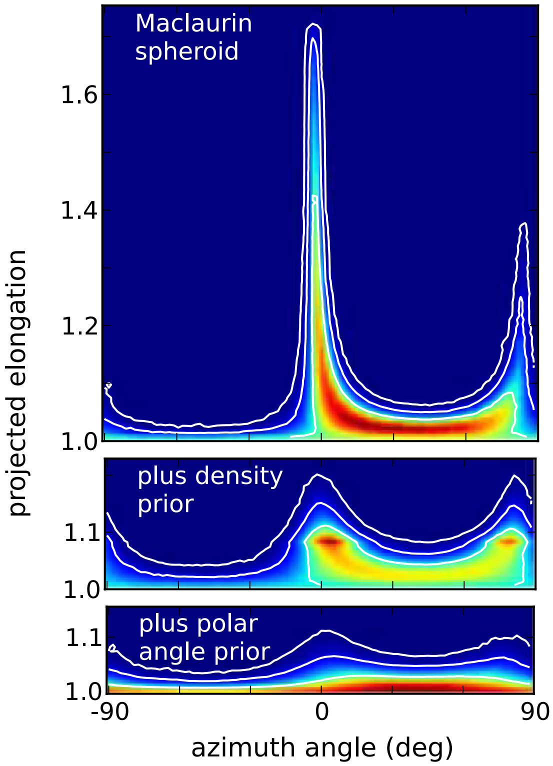

Figure 3. Two-dimensional probability densities of azimuth angle vs. projected elongation (the projected elongation PDFs of Figure 1 are integrals of these two-dimensional functions over azimuth angle). In the Maclaurin spheroid fit and the fit with the density prior added, the highest probability density regions have either low elongation or have a elongation aligned in the unconstrained north–south direction. Note that both angles near 0°—with their major axis aligned north–south—angles near ±90°—with their minor axis aligned north–south—result from this lack strong north–south constraint. Both configurations yield acceptable fits (see Figure 1). If the polar angle is assumed to be small, the preference for north–south elongation nearly disappears as the projected elongation is small.

(A color version of this figure is available in the online journal.)

using our prior knowledge that we are looking at a two-dimensional projection of an arbitrarily oriented Maclaurin spheroid, this analysis provides a three times tighter constraint on the measured projected elongation than the O12 1σ upper limit of 1.32. Our PDF for ϕ is not as would be expected for a random orientation, but rather has a peak and 1σ range of 20^{+40}_{-8}.

These results correctly take into account both the constraints from the data and the geometric expectations of a randomly oriented projected ellipse. Knowing that the Maclaurin spheroid can have a wide range of values for E between 1 and 1.716, the pole position must be close to the line of sight or else a larger projected elongation would be measured, *or* the elongation must be close to the north–south direction where the elongation is unconstrained. But, because the volume of parameter space is low in the unconstrained direction, the overall likelihood of this orientation and thus these large elongations is small. Figure 3 illustrates this effect by showing probability contours of elongation azimuth versus projected elongation.

4. FIT TO RADIOMETRIC AND DENSITY CONSTRAINTS

We now add prior constraints to help us determine the projected shape. We first use the combined Spitzer and Herschel radiometry which suggests that the projected area of Makemake is 1420 ± 60 km (Lim et al. 2010). This prior mainly serves to limit very large elongations in the north–south direction which would cause the thermal emission to be higher than observed.

A more important prior is on the density. While above, we allowed E to range between 1 and 1.716—essentially choosing a uniform prior for the elongation—a more physically motivated approach is to use a prior on the density itself, rather than the elongation, and allow the density and rotation period to determine the elongation.

O12 claim that their occultation results provide a measurement of the density of Makemake of 1.7 ± 0.3 g cm^{-3}. The primary justification for the assumption of a density of 1.7 ± 0.3 g cm^{-3} is that for higher densities, the volatile retention models of Schaller & Brown (2007; Brown et al. 2011, updated in) predict retention of N_2 for a body of the size and temperature of Makemake, which would then result in a measurable atmosphere in the O12 occultation data. This statement is, however, a gross misinterpretation of the volatile retention models. In the models of Schaller & Brown (2007), we explicitly and deliberately calculate the *slowest* possible volatile loss mechanism—Jeans escape—so that objects that would lose all of their volatiles due to this mechanism must have lost all of their accessible volatiles. But it is incorrect to say that objects which could have retained volatiles against Jeans escape must have retained them against all other mechanisms. Haumea is an excellent example. Based on its size, mass, and temperature, it could easily hold its volatiles against Jeans escape over the life of the solar system. Another process, however, presumably a giant impact (Brown et al. 2007), led to complete volatile loss. The arguments of O12 would instead state that the lack of CH_4 on Haumea constrains its density to be ∼1 g cm^{-3}, rather than its measured value of ∼2.6 g cm^{-3} (Rabinowitz et al. 2006)! These arguments for the density constraint on Makemake based on the absence of a detectable atmosphere are clearly spurious and should be given no weight.

The O12 lower limit to the density of 1.4 g cm^{-3} comes from using the same volatile retention models to explain the continued presence of CH_4 on the surface. Here the volatile loss model is used correctly. For densities below 1.4 g cm^{-3} Makemake must have lost all of its CH_4 even if the only escape process was slow Jeans escape. We retain this lower limit as a sensible constraint.

The upper limit to the density from O12 comes from assuming that the inferred value of 1.7 g cm^{-3} is close to correct and positing that objects of similar size have densities within about 0.3 g cm^{-3} of that value. Use of this upper limit is problematic. The most important question to address about the density of Makemake is whether it has a value below about 2.1 g cm^{-3}, as might be typical for objects with large, potentially captured satellites, or a higher value as might be typical for objects with evidence for giant impacts. Assuming that the upper limit to the density of Makemake is 2.0 g cm^{-3} simply asserts an answer to that question, which is clearly unacceptable.

Based on these considerations, we retain the 1.4 g cm^{-3} lower limit based on the retention of CH_4 (though we employ a softer cutoff by assuming a one-sided Gaussian distribution with a σ of 0.03 for densities below 1.4 g cm^{-3}), and we add the only reasonable upper limit density that we can find, which is that the density is certainly—we assume—below that of solid rock or about 3.2 g cm^{-3}. We see no justification for placing any other prior constraints on the density of Makemake, so from 1.4 to 3.2 g cm^{-3} we assume a uniform prior.

Once again employing our MCMC integration, we find that when using the density prior the PDF for the projected elongation peaks strongly at 1.0, with a 1σ upper limit of 1.06

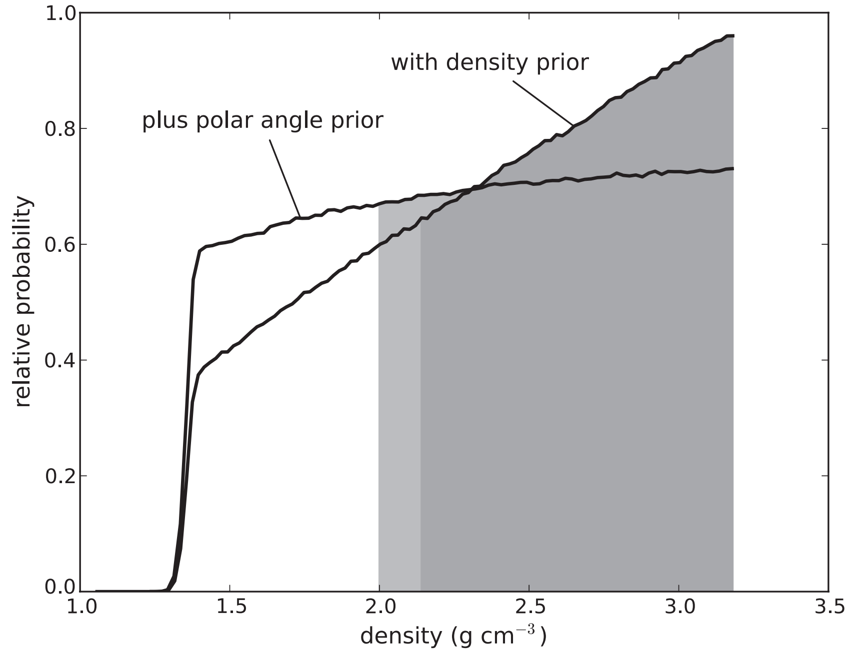

Figure 4. PDF for density. The prior on density is uniform from 1.3 to 3.2 g cm^{-3}. The occultation data suggest that higher densities are preferred owing to their smaller true elongations, but, as the PDF shows, the constraint is nearly meaningless. Adding the prior that Makemake is viewed nearly pole-on puts less constraint on the elongation and thus on the density. The density PDF very nearly resembles the original prior in this case, showing that, again, the density is unconstrained by the occultation data.

Table 1
Derived Properties of Makemake

Parameter	Sphere	Maclaurin Spheroid	Plus Density Prior	Plus Polar Angle Prior
Projected elong	1.00	<1.09	<1.06	<1.02
Actual elong, E	1.00	<1.37	$1.077 < E < 1.12$	$1.077 < E < 1.13$
Equatorial diameter (km)	1430 ± 14	1432^{+84}_{-24}	1434^{+48}_{-18}	1434 ± 14
Projected polar diameter, d (km)	n/a	1424^{+16}_{-14}	1420^{+18}_{-24}	1422 ± 14
Actual polar diameter (km)	n/a	1420^{+20}_{-240}	1320^{+40}_{-60}	1320^{+20}_{-60}
Albedo	0.80 ± 0.01	$0.80^{+0.05}_{-0.07}$	$0.81^{+0.03}_{-0.05}$	$0.81^{+0.01}_{-0.02}$
Polar angle, ϕ (deg)	n/a	20^{+40}_{-8}	32^{+23}_{-19}	19 ± 11*
Density	n/a	n/a	>2.14*	>1.98*

Note. * Result dominated by prior

(Figure 2). The smaller elongation derived here is the result of the 1.3 g cm^{-3} lower limit on the density, which, for a 7.77 hr rotation period, translates to an upper limit to the true elongation, E, of 1.20. For the same reason, the polar axis angle is not as strongly constrained to small values, and we find a best fit at 32^{+23}_{-19}. The projected polar diameter has values of 1420^{+18}_{-24} km. By calculating the PDF of the projected area and comparing it to the results of O12, we also calculate an albedo PDF with a distribution peak and range of $0.81^{+0.03}_{-0.05}$.

The PDF for the density rises linearly from 1.4 to 3.2 g cm^{-3} (Figure 4). We can derive a formal 1σ lower limit to the density of 2.14 g cm^{-3}, but this lower limit is meaningless, as the distribution of the density is just the density prior modified to have a slight preference for less elongation and thus higher densities. The data themselves provide nearly no constraint on the density.

5. POLAR AXIS CONSTRAINTS

As discussed by O12, there is reason to believe that we are viewing Makemake nearly pole-on. Spitzer radiometry can only be fit by assuming that the surface of Makemake—like that of Pluto—contains a combination of very high and very low albedo regions (Stansberry et al. 2008; Lim et al. 2010), yet Makemake shows only a 0.03 magnitude variation over its 7.77 hr rotation period (Heinze & de Lahunta 2009). Either the dark regions of Makemake must be extremely symmetric with respect to the pole, which is not the case for the similarly mottled Pluto (Buie et al. 2010) and requires special pleading, or we are viewing Makemake from a nearly pole-on position.

Adding a prior on the pole position of Makemake strongly affects the results, yet there is no obvious statistical distribution that one should adopt. We make a judgement based on the evidence above that the polar axis angle is likely less than 20°. We quantify this as a prior on polar axis angle of the form of a Gaussian distribution peaked at 0°, with a σ of 20°. This prior is in addition to the prior that the axes are otherwise randomly oriented in space. The specific values cannot be statistically justified, but will nonetheless serve as an instructive example of how to incorporate our expectations of the polar angle.

Once again we construct the six-dimensional PDF from an MCMC analysis. We find, not surprisingly, that the polar axis angle is much more tightly confined to small angles, with the PDF peak and range of 19 ± 11. The projected polar radius has a value of 1422 ± 14 km, while the albedo is constrained to $0.80^{+0.02}_{-0.01}$. The density remains nearly unconstrained, with a PDF that again rises linearly from 1.4 to 3.2 g cm^{-3} (Figure 4). With our prior expectation of a small polar angle, there is less of a bias toward high densities, as small polar angle gives small projected elongations regardless of the real elongation. In this case the formal 1σ lower limit on the density is 1.98 g cm^{-3}, but, as before, the constraint is dominated by the prior and the data themselves give little information on the density. Table 1 summarizes the results of these analyses.

6. CONCLUSIONS

We have developed a new statistically rigorous approach to the analysis of dwarf planet occultation data which incorporates our knowledge of shapes of equilibrium, spherical geometry, and volatile retention to place statistically justifiable limits on the shapes of these objects. We apply the new technique to the occultation of Makemake observed by Ortiz et al. (2012), which was initially analyzed using a combination of quantitative and qualitative approaches. We find that the "preferred" solution of Ortiz et al. (2012) for the elongation of Makemake is unjustified and leads to incorrect estimates of the precise dimensions and albedo of Makemake. In our solution in which we use the inference from photometric data that Makemake is being viewed nearly pole-on, we find a 1σ upper limit to the projected elongation of Makemake of 1.02, with measured equatorial diameter of 1434 ± 14 km and a projected polar diameter of 1422 ± 14 km, yielding an albedo of $0.81^{+0.01}_{-0.02}$. If we remove the external constraint on the pole position of Makemake, we find instead a 1σ upper limit to the elongation of 1.06, with a measured equatorial diameter of 1434^{+48}_{-18} km and a projected polar diameter of 1420^{+18}_{-24} km, yielding an albedo of $0.81^{+0.03}_{-0.05}$.

The uncertainties reported here (and by O12) are purely statistical. True shape uncertainties are also affected by deviations from our modeled equilibrium shapes. Our best knowledge of the shapes of icy bodies of this diameter comes from the medium-sized icy moons of Saturn. With the exception of Iapetus, for which a complex thermal and rotational history within the Saturnian system has been evoked, deviations from equilibrium shapes of like-sized Saturnian satellites are of the order of 1 km (Thomas et al. 2007). Such shapes are well below our statistical errors and so do not strong affect the reported results.

The density measurement of Ortiz et al. (2012) is based on misapplication of the volatile retention models of Schaller & Brown (2007) and arbitrary assumptions about plausible densities. Unfortunately, while the occultation measurements of O12, when analyzed correctly, provide excellent constraints on the size, shape, and albedo of Makemake, they contain essentially no information about density of this object. The density of Makemake, while an important parameter for understanding the evolution of the population of dwarf planets, remains unknown.

REFERENCES

Brown, M. E. 2008, in The Solar System Beyond Neptune, ed. M. A. Barucci, H. Boehnhardt, D. P. Cruikshank, & A. Morbidelli (Tucson, AZ: Univ. Arizona Press), 335
Brown, M. E. 2012, AREPS, 40, 467
Brown, M. E., Barkume, K. M., Ragozzine, D., & Schaller, E. L. 2007, Natur, 446, 294
Brown, M. E., Burgasser, A. J., & Fraser, W. C. 2011, ApJL, 738, L26
Brown, M. E., van Dam, M. A., Bouchez, A. H., et al. 2006, ApJL, 639, L43
Buie, M. W., Grundy, W. M., Young, E. F., Young, L. A., & Stern, S. A. 2010, AJ, 139, 1128
Chandrasekhar, S. 1969, Ellipsoidal Figures of Equilibrium (New Haven, CT: Yale Univ. Press)
Foreman-Mackey, D., Hogg, D. W., Lang, D., & Goodman, J. 2012, arXiv:1202.3665
Goodman, J., & Weare, J. 2010, Commun. Appl. Math. Comput. Sci., 5, 65
Heinze, A. N., & de Lahunta, D. 2009, AJ, 138, 428
Lim, T. L., Stansberry, J., Müller, T. G., et al. 2010, A&A, 518, L148
Ortiz, J. L., Sicardy, B., Braga-Ribas, F., et al. 2012, Natur, 491, 566
Rabinowitz, D. L., Barkume, K., Brown, M. E., et al. 2006, ApJ, 639, 1238
Schaller, E. L., & Brown, M. E. 2007, ApJL, 659, L61
Stansberry, J., Grundy, W., Brown, M., et al. 2008, in The Solar System Beyond Neptune, ed. M. A. Barucci, H. Boehnhardt, D. P. Cruikshank, & A. Morbidelli (Tucson, AZ: Univ. Arizona Press), 161
Thomas, P., Burns, J., Helfenstein, P., et al. 2007, Icar, 190, 573